Title

Automated single-cell proteomics providing sufficient proteome depth to study complex biology beyond cell type classifications

Authors

Claudia Ctortecka[1], Natalie M. Clark[1], Brian Boyle[1], Anjali Seth[2], D. R. Mani[1], Namrata D. Udeshi[1] & Steven A. Carr[1]

Affiliation

1 Broad Institute of MIT and Harvard, 415 Main Street, 02142 Cambridge, MA, USA.

2 Cellenion SASU, 60F avenue Rockefeller, 69008 Lyon, France.

Correspondence

Steven A. Carr

scarr@broad.mit.edu

Broad Institute of MIT and Harvard
415 Main Street
02142 Cambridge
MA, USA.

Abstract

Mass spectrometry (MS)-based single-cell proteomics (SCP) has gained massive attention as a viable complement to other single cell approaches. The rapid technological and computational advances in the field have pushed the boundaries of sensitivity and throughput. However, reproducible quantification of thousands of proteins within a single cell at reasonable proteome depth to characterize biological phenomena remains a challenge. To address some of those limitations we present a combination of fully automated single cell sample preparation utilizing a dedicated chip within the picolitre dispensing robot, the cellenONE. The proteoCHIP EVO 96 can be directly interfaced with the Evosep One chromatographic system for in-line desalting and highly reproducible separation with a throughput of 80 samples per day. This, in combination with the Bruker timsTOF MS instruments, demonstrates double the identifications without manual sample handling. Moreover, relative to standard high-performance liquid chromatography, the Evosep One separation provides further 2-fold improvement in protein identifications. The implementation of the newest generation timsTOF Ultra with our proteoCHIP EVO 96-based sample preparation workflow reproducibly identifies up to 4,000 proteins per single HEK-293T without a carrier or match-between runs. Our current SCP depth spans over 4 orders of magnitude and identifies over 50 biologically relevant ubiquitin ligases. We complement our highly reproducible single-cell proteomics workflow to profile hundreds of lipopolysaccharide (LPS)-perturbed THP-1 cells and identified key regulatory proteins involved in interleukin and interferon signaling. This study demonstrates that the proteoCHIP EVO 96-based SCP sample preparation with the timsTOF Ultra provides sufficient proteome depth to study complex biology beyond cell-type classifications.

Introduction

Genomics, transcriptomics and imaging methods with single-cell resolution have been shown to provide new insights to the complex cellular interplay that underlies development and disease[1–3]. Currently, most single-cell approaches aim at resolving biological heterogeneity by describing diverse sub-populations or unexpected cell types within a given sample[4,5]. In the past few years, single-cell proteomics (SCP) has developed into a viable complement to other sequencing-based omics techniques[6–11]. Mass spectrometry (MS)-based proteomics is ideally suited to study cellular identity and functionality as those are mostly driven by proteins or their post-translational modifications (PTMs)[12,13]. Until recently, the limited protein content of most mammalian cells, which is only about 50-300 pg, represented a significant challenge to MS-based SCP[14]. Even though this is over 1000 times lower than standard input of current MS-based proteomics studies, the latest advances in dedicated workflows and liquid chromatography tandem mass spectrometry (LC-MS/MS) instrumentation have begun to overcome these sensitivity limitations[15–24]. Recent SCP studies enabled the identification and quantification of thousands of proteins from a single-cell in contrast to earlier reports that relied on chemical multiplexing of multiple single-cells to reach the limit of detection[7,18,25]. These strategies, however suffer from inherent reporter ion signal suppression or ratio compression of isobaric labels, in standard data dependent (DDA) acquisition, which negatively impacts quantitative accuracy[26–28]. Additionally, stochastic precursor selection in DDA results in missing data when analyzing large numbers of single-cells in multiple TMT plexes[10,29–31].

Pioneering studies demonstrated reproducible in-depth profiling of one single mammalian cell at a time through optimization of sample preparation, chromatographic separation, data acquisition and data analysis[10,25,29–34]. While label-free quantification of individual cells does not suffer from interferences related to isobaric labeling, measurement throughput is significantly decreased[35]. Moreover, multiple avenues have been pursued to increase the acquisition throughput while providing the most complete proteome profiles across relatively large sample sets[23,36]. Some of these include the use of dual columns to simultaneously elute peptides of one analytical column while the other is washed and equilibrated for the subsequent sample. Additionally, high-flow and high-pressure column loading or trap-and-elute setups are used to reduce the overhead time between active peptide elution. Recently, non-isobaric labels (up to 3-plex) have been implemented in combination with rapid data independent acquisition (DIA) to multiplex cells per analytical run but minimize signal interference and reduce missingness[15,37]. DIA follows a pre-defined acquisition pattern, theoretically fragmenting the same precursor sets in every sample. In

contrast to DDA, only precursors that match specific selection parameters (i.e. charge state or intensity) are tightly isolated and individually fragmented according to a one scan, one peptide scheme. To achieve necessary acquisition speed, most DIA isolation windows are wider than in DDA methods, therefore multiplexing multiple precursors in one scan. This makes DIA, relative to DDA data, inherently more difficult to analyze. However, capitalizing on the trapped ion mobility separation (TIMS) technology of the Bruker timsTOF instruments, several SCP-DIA approaches have shown great potential[10,15,37]. Those dedicated diaPASEF strategies allow one to focus on the most productive precursor population (i.e. 400-1000 m/z), while excluding most singly charged contaminating ions.

The interpretation of convoluted DIA spectra rely on efficient chromatographic separation and reproducible sample preparation across large sample sets to minimize missing values[38–40]. Manual sample handling and transfer between reaction vessels, especially at the ultra-low input levels, can decrease reproducibility and peptide recovery, negatively impacting the ability to obtain biological meaningful data[32,41]. To eliminate manual sample handling, we here benchmark a fully automated workflow for label-free low nanoliter SCP sample preparation using the proteoCHIP EVO 96 with the picolitre and single cell dispensing robot, the cellenONE®. Similar to other successful SCP sample processing workflows like the nanoPOTS[9], nPOP[42], OAD[11], the proteoCHIP 12*6[18] or plate based methods[8], we utilize a ‘one-pot approach’ where all buffers and chemicals are sequentially added to the single cell. More recent developments have demonstrated that direct integration of the sample preparation vessel with the HPLC further increases reproducibility and peptide recovery[18,42–45]. However, these ‘one-pot approaches’ still contain all side products and excess of chemicals used for sample preparation in each ‘pot’. To remove the sample background efficiently and reproducibly we have therefore seamlessly integrated the proteoCHIP EVO*96 to the high throughput chromatography system, the Evosep One[36]. In contrast to most standard HPLC systems, the Evosep One implements disposable trap columns for in-line sample cleanup prior to LC-MS/MS analysis. This has been demonstrated to greatly increase chromatographic throughput, reproducibility, and sensitivity in conjunction with rapid MS acquisition[10,43,45,46].

Here we combine the automated sample handling of the proteoCHIP EVO 96, high peak capacity of the nanoflow Evosep One methods and optimal ion usage of the Bruker timsTOF instruments into a novel integrated workflow for label-free SCP. To showcase the performance of our workflow relative to previously published methods, we demonstrate its applicability with the standard cell-line HEK-293T and recapitulate effects of LPS treatment in hundreds of single THP-1 cells.

Results

The automated proteoCHIP EVO 96 SCP workflow minimizes adsorptive peptide losses

The proteoCHIP EVO 96 is a micromachined low-adsorptive PTFE chip with conical nanowells in the layout of a 96-well plate (Figure 1a; proteoCHIP EVO 96). For sample processing, the proteoCHIP EVO 96 is inserted into the cellenONE®. For simultaneous lysis and digestion, we used a master-mix (MM) comprised of a MS-compatible detergent (DDM, 0.2%), a protease (trypsin, 10 ng/µL) and a buffer (TEAB, 100mM) as described in our previous TMT-based multiplex workflow[18]. To ensure successful deposition of the single cells within the MM droplet, we initially dispensed 150 nL MM, followed by the isolated cell, which was subsequently covered by another 150 nL MM. To reduce evaporation, the SCP workflow was performed at 80% humidity within the cellenONE®. Prior to lysis and digestion, 3 µL of hexadecane was dispensed in each nanowell. Lowering the chip temperature to 10 °C causes the hexadecane to solidify (melting point: 18.18 °C), providing a flat working surface within each conical proteoCHIP nanowell. During cell lysis and protein digestion, the temperature on deck within the cellenONE® was increased to 45 °C, melting the hexadecane and fully submerging the cell in the MM. To enforce mixing and improve cell lysis, 50 nL H_2O was automatically added to the nanowells every 2 minutes for the full 2-hour incubation time (detailed in materials and methods). All processing steps of this ‘one pot’ workflow was carried out within each nanowell reducing adsorptive losses due to pipetting or transfer of the sample. For direct transfer of the SCP sample to the autosampler, the proteoCHIP EVO 96 was designed to fit on top of a box of Evotips. The chip was inverted to fit each nanowell (i.e. one SCP sample) on top of each Evotip, which are disposable trap columns for in-line desalting within the Evosep One HPLC system (Fig. 1a). Through centrifugation the digested peptides in solution were transferred to the tips, the now empty proteoCHIP EVO 96 was removed from the Evotip box, all Evotips were washed within the centrifuge and then directly placed on the Evosep One for chromatographic separation (Fig. 1a). This workflow can be performed utilizing a full proteoCHIP preparing 96 single-cells at a time or only a partial chip, depending on the experimental requirements.

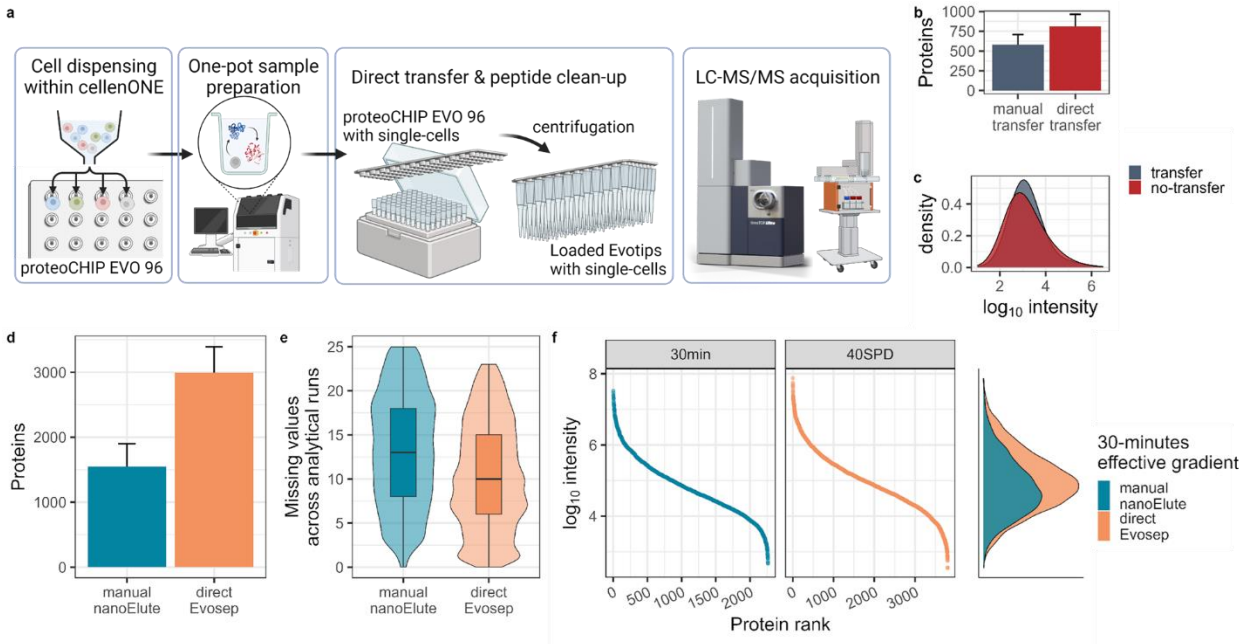

Fig. 1: Direct sample transfer to Evotips improves peptide recovery. (a) Schematic overview of the proteoCHIP EVO 96 workflow, including cell dispensing, lysis, protein digestion, transfer of single cells to Evotips and loading Evotips to the timsTOF SCP. Bar represents median and error bar indicates Median Absolute Deviation (MAD). (b) Protein identifications and (c) precursor abundance of HEK293T single cells upon manual (gray) or direct transfer via centrifugation (red) in ddaPASEF acquisition. n = 10 (d) Protein identifications from single cells after manual transfer to HPLC vials with the nanoElute (blue) or direct transfer to the disposable trap columns, the Evotips (orange) acquired in diaPASEF on the timsTOF SCP. Bar indicates median and error bar the MAD. (e) Missing quantitative values per precursor and (f) ranked $\log_{10}$ intensity of single-cells upon 30-minutes effective gradient on the nanoElute with manual transfer (blue) or the Evosep (i.e. 40SPD; orange) with direct transfer. n = 50.

To evaluate the impact of sample transfer on peptide recovery, we initially carried out one proteoCHIP EVO 96 workflow and then transferred 5 cells by manually pipetting cell samples to Evotips, while another 5 cells were transferred via centrifugation as described above (Fig. 1a). We then analyzed those samples on the timsTOF SCP with a ~30-minute effective nanoflow gradient on the Evosep One (40 samples per day, SPD Whisper). The manually transferred samples yielded a median of 582 proteins per analytical run, while the direct loading of the Evotips resulted in a median of 812 proteins per single-cell. This indicated that automated transfer of the sample increased protein identifications by 29% in comparison to the manually pipetted ones (Fig. 1b). Additionally, while no peptides with specific hydrophobicity index (GRAVY) were lost with pipetting, the direct transfer recovered lower abundant peptides (Fig. 1c, Supplemental Fig. 1a)[47].

This demonstrates the impact of peptide adsorption at single-cell input levels and the benefit of direct sample transfer through the dedicated design of the proteoCHIP EVO 96.

Next, we further optimized the timsTOF acquisition method based on the default tryptic ddaPASEF acquisition strategy used in Fig. 1b-c. We adapted a low-input diaPASEF method to the 4 sec wide Full-Width-Half-Maximum (FWHM) elution peaks obtained with 40SPD using the IonOpticks Aurora 15 cm columns, on average resulting in 7 points across the peak. To benchmark the improvement in performance relative to the standard nanoElute LC system, we prepared single-cells with the proteoCHIP EVO 96 workflow, manually transferred 25 cells to HPLC vials for 30-minutes effective gradient on the nanoElute or directly loaded 25 cells to Evotips, as described above, for 40SPD (Fig. 1a). The standard nanoElute separation on the same column yielded 1,547 proteins on average per single-cell (Fig. 1d). Using the modified diaPASEF acquisition method, together with the 40SPD method, we identified 3,000 proteins per single HEK-293T cell (Fig. 1d). This highlighted that the combination of direct loading of samples onto Evotips together with the 40SPD Evosep One separation method recovered about 2-fold more proteins and increased sample throughput by 30% in contrast to the 30-minutes effective gradient on the nanoElute (i.e. 30-minutes effective gradient plus 20 minutes loading and column equilibration).

Lastly, we sought to evaluate the differences in data completeness and dynamic range obtained using the direct Evosep- versus the manual nanoElute method for proteoCHIP EVO 96-based single-cell samples (Fig. 1e, f). For this we compared the number of missing quantitative values per precursor across all 25 single-cells (i.e. analytical runs) acquired on the Evosep or the nanoElute. We observed 12% more data completeness using the directly transferred Evosep samples compared to the manual nanoElute approach (Fig. 1e). This paralleled the loss of low abundant peptide signals after manual sample transfer and the decreased protein identifications with nanoElute separation (Fig. 1c-e). In addition to increased peptide recovery and reduced missingness, the directly transferred Evosep samples showed a similar dynamic range compared to the manual nanoElute ones (Fig. 1e-f). Using the manual nanoElute or the direct Evosep method, SCP samples prepared with the proteoCHIP EVO 96 spanned close to 5 orders of magnitude with similar peptide moieties (Fig. 1f, Supplemental Fig. 1b). Interestingly, in contrast to ddaPASEF acquisition, precursor abundance acquired with diaPASEF was higher in the direct Evosep SCP samples compared to the manual nanoElute (Fig. 1 c,f). This is in contrast to the broader nanoElute peaks with an average FWHM of 5.1 seconds, which results in more co-eluting peptides and more convoluted spectra. Based on this we hypothesize that the increased speed

of the dedicated diaPASEF acquisition strategy in combination with the high peak capacity of the 40SPD allowed us to sample precursors more efficiently across the entire dynamic range (Fig. 1f).

Doubling the SCP acquisition throughput still identifies biologically relevant proteins

Most standard SCP projects require the acquisition of hundreds to thousands of single cells to resolve tissue or population heterogeneity and to understand the underlying biology. However, shorter chromatographic separation time challenged acquisition speed and effective ion usage of the timsTOF SCP. Therefore, for subsequent experiments we implemented the timsTOF Ultra, which is equipped with a 'brighter' ion source and a higher capacity TIMS cartridge[48]. The combination of the larger inner diameter glass capillary and concomitant increased gas flow into the instrument allows for more efficient ion usage compared to the timsTOF SCP. This was reflected by the identification of over 3,500 proteins per single cell with the 40SPD method, which is 15% higher compared to single cells acquired on the timsTOF SCP (compare Fig. 1d to Fig. 2a). For our comparative studies we combine only single cells without the usage of a carrier sample for data analysis to eliminate the possibility of identification transfer without controlling the false discovery rate across the entire dataset[49,50].

Next, to realistically carry out studies including hundreds or thousands of single cells we aimed at doubling the acquisition throughput using a 15-minute effective gradient nanoflow Evosep method. This dedicated high throughput method on the Evosep enables analysis of 80 samples per day (SPD) at 100 nL/min in conjunction with the 5 cm IonOpticks Aurora Rapid column. To minimize technical variability for comparing the separation lengths, we performed one proteoCHIP EVO 96 SCP workflow, acquired 48 single-cells with the high throughput 80SPD method, replaced the 5 cm Aurora Rapid column with the 15 cm Aurora Elite column and resumed acquisition of the remaining 48 single-cells using the 40SPD method on the timsTOF Ultra. As expected, with the short 80SPD separation method the median number of proteins identified decreased to 1,200 per single cell, representing a drop of ~60% compared to 40SPD (Fig. 2a). Importantly, nearly all the proteins identified with the 80SPD were also identified in the 40SPD method, which demonstrates the reproducibility of our SCP workflows and acquisition strategies (Fig. 2b).

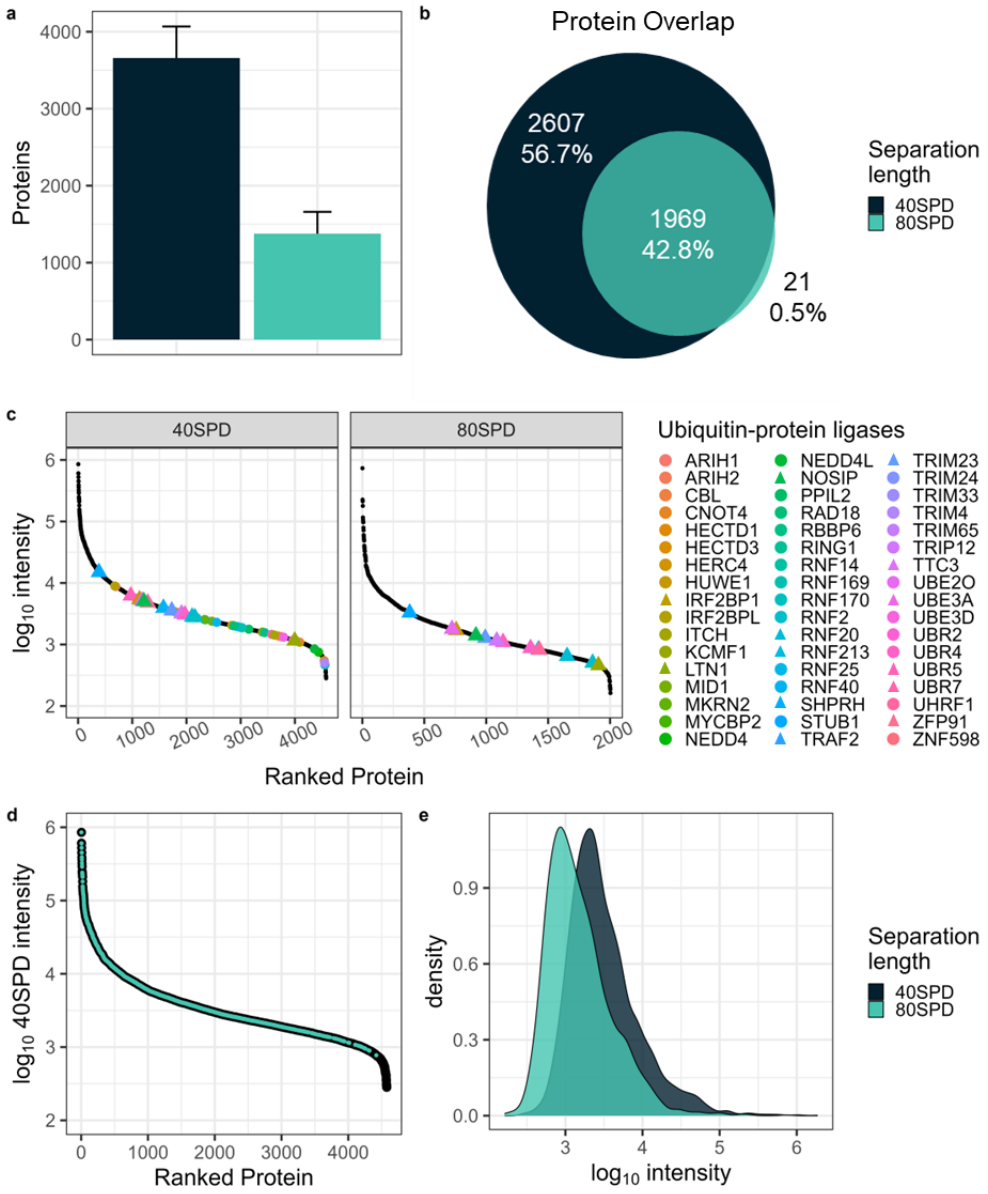

Fig. 2.: Doubling sample throughput reduces proteome depth but still identifies biologically relevant proteins. (a) Protein identifications of single cells prepared with the proteoCHIP EVO 96 and acquired on the timsTOF Ultra at 40SPD (black; n = 48) or 80SPD (turquoise; n = 48) in diaPASEF. n = 96. Bar indicates median and error bar MAD. (b) Protein identification overlap of single cells acquired with 40SPD (black) or 80SPD (turquoise). (c) Ranked $\log_{10}$ intensity of proteins identified in 40SPD and 80SPD. Colored points represent 51 biologically-relevant ubiquitin-protein ligases. Targets of interest that are recovered in both 40SPD and 80SPD are indicated with a triangle. (d) $\log_{10}$ intensity of single cells acquired with 40SPD (black) overlaid with proteins also identified with 80SPD (turquoise). (e) Density distribution of $\log_{10}$ intensity of single cells acquired at 40SPD (black) or 80SPD (turquoise) in diaPASEF on the timsTOF Ultra.

Next, we investigated the overall abundance of quantified proteins using both the 40SPD and the 80SPD methods. The increased throughput using the 80SPD separation method reduced the dynamic range of single-cell analysis by one order of magnitude (Fig. 2c). We sought to understand the impact of this reduction on protein identification and quantification with a focus on ubiquitin-protein ligases, a protein family of high biological interest. These ligases are highly diverse key players in cell cycle, signaling and cellular homeostasis balancing health and disease[51–54]. Using the 40SPD method, we identify over 50 ubiquitin ligases in single cells while 13 are recovered using the 80SPD method (Fig. 2c). While the intensity of the ligases detected using the 80SPD method were reduced by close to one order of magnitude, the rank order of abundance remained the same between the two methods (Fig. 2c). Based on the reduced number of identifications and dynamic range using the 80SPD method, but the almost complete overlap of proteins identified, we speculated that the proteins we did not observe were of lower abundance. Indeed, proteins with an MS1 abundance of less than 1e3 in 40SPD generally dropped below the limit of detection in 80SPD (Fig. 2d). Additionally, more frequent co-isolation of precursors in shorter gradients increases the complexity of MS/MS scans for identification and can result in signal suppression of lower by higher abundant precursors (Fig. 2e). This demonstrates that 2-fold higher single-cell analysis throughput is feasible, at decreased analysis depth. Therefore, the experimental design must take into consideration whether the acquisition of hundreds or thousands of single cells are required for statistical significance and if the proteins of interest can still be reliably quantified to address the specific biological question.

Lipopolysaccharide-induced proteome changes are validated in single cells

Lipopolysaccharide (LPS) is known to stimulate inflammation, produce cytokines and activate metabolic responses in a wide range of cells[55–57]. We aimed to evaluate whether our proteoCHIP EVO 96-based SCP workflow can be used to profile the effects of LPS stimulation at the single-cell level. For this, we treated a commonly used human leukemia monocytic cell line (THP-1) with 200 ng/mL of LPS (n = 77) and a DMSO control (n = 84) for 12 hours. The exposure of THP-1 cells to LPS is known to induce inflammatory cytokines, activate the tumor necrosis factor (TNF) pathway and radical oxygen species production[56,58]. The treated cells were processed with our proteoCHIP EVO 96 workflow, transferred to Evotips and data were acquired with the 40SPD method on the timsTOF Ultra (Fig. 3a). The LPS treatments were performed in process duplicates with 48 single-cells per condition and proteoCHIP EVO 96, each starting from a distinct THP-1 cell passage. The two batches were processed with separate but identical proteoCHIP EVO 96 workflows and acquired on the timsTOF Ultra on different days (Supplemental table 1). We identified up to 1,537 proteins with a median of 1,149 proteins per single-cell (Fig. 3b). The

nominal decrease in identifications per single cell compared to the HEK-293T cells displayed in Fig. 2a is due to the 2-fold decreased cell size (Fig. 2a, Fig. 3b; Supplemental Fig. 2).

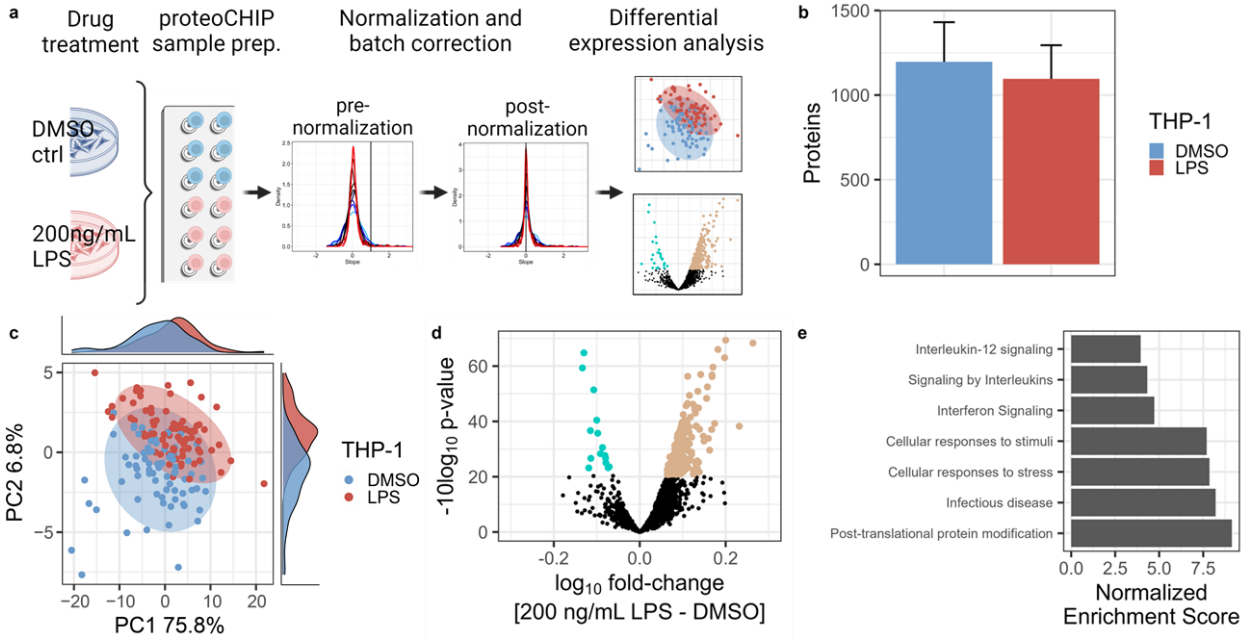

Fig. 3.: proteoCHIP EVO 96 SCP sample preparation reflects expected proteome changes THP-1 cells upon LPS treatment. (a) Schematic overview of the proteoCHIP-based workflow, including LPS treatment of THP-1 cells, unsupervised cluster normalization and batch correction followed by differential expression analysis. (b) Protein identifications and (c) PCA of single cells prepared with the proteoCHIP EVO 96 and acquired on the timsTOF Ultra at 40SPD upon 12 hours of 200 ng/mL (n=84) LPS or DMSO (n = 77) treatment. Bar represents median and error bar MAD. Ellipse represents 95% confidence interval. (d) Volcano plot of two-sample *t*-test results (200 ng/mL LPS over DMSO). Log_{10} fold change and $-10log_{10}$ p-value are shown, significantly regulated proteins with an adjusted p-value ≤0.05 are indicated in blue (down, 15 proteins) and brown (up, 214 of proteins). (e) Normalized Enrichment Scores (NES) of significantly enriched Reactome pathways identified by Gene Set Enrichment Analysis (GSEA) on two-sample *t*-test results. All shown pathways are statistically significant with adjusted p-value < 0.01.

Compared to bulk proteomics data, SCP datasets exhibit distinct considerations for normalization, due to technical variability throughout the sample processing, or differences in cell size[59,60] (Supplemental Fig. 2; HEK-293T – 26.7 µm, THP-1 – 13.7 µm). Thus, we normalized our single-cell proteomics data using SCnorm[61], which is an approach originally developed for single-cell transcriptomics studies (Fig. 3a; Supplemental Fig. 3). Normalized single-cell abundances were then log_{10}-transformed and batch-corrected using limma as we observed that approximately 7% of the total variance was due to technical batch effects from processing the cells on different days (Supplemental Fig 4). Principal Component Analysis (PCA) on the normalized, batch-corrected data shows a separation between the two treatment groups across the first (PC1, 75.8%

explained variance) and second principal components (PC2, 6.8% explained variance; Fig. 3c). We identified 214 proteins as significantly upregulated in the LPS treated cells while 15 were significantly downregulated compared to the DMSO control (Fig. 3d; moderated two-sample t-test, 229 significant proteins, adj. p-value ≤ 0.05). To evaluate the biological significance of these proteins, we performed Gene Set Enrichment Analysis (GSEA[62]) on the MSigDB Reactome gene sets. The top positively enriched pathways upon LPS treatment modulate proteins implicated in Interferon signaling as well as inflammatory pathways such as Interleukin signaling and specifically the Interleukin-12 family, which is consistent with the known role of LPS[63,64] (Fig. 3e).

Additionally, we compared our results to a previous in-depth proteomics analysis of THP-1 cells treated with LPS for 12 hours[56]. We validated concordant fold-change in protein expression of key response proteins, such as the anti-oxidative response to increased intracellular ROS through elevated levels of HMOX1[58] (Supplementary Fig. 5). Moreover, we find the cytokine molecule CLEC11A to be slightly elevated in the LPS treated cells compared to the DMSO control (Supplementary Fig. 5)[65]. It has been postulated that CLEC11A is actively secreted from the THP-1 cells during LPS stimulation and becomes less abundant upon prolonged (longer than 6-hours) LPS exposure[56], which provides a possible explanation for the slight elevation of CLEC11A in this study.

Discussion

We present an automated label-free SCP workflow through the combination of a novel proteoCHIP design and sample preparation, high-throughput chromatography, dedicated acquisition methods and latest computational advances. The commercially available proteoCHIP EVO 96 SCP workflow is automated within the cellenONE® with minimal user guided operations. The temperature and humidity-controlled incubation and all nanoliter pipetting steps are performed within the cellenONE® via automated scripts. This aims at making efficient SCP workflows more accessible to the general proteomics audience and diverse core facilities. Moreover, the direct interface with the disposable trap columns, the Evotips, allow for sensitive and reproducible chromatographic separation with standardized protocols. We demonstrate that including a single manual sample transfer step reduces protein identifications by 29%, and those losses are increased to over 49% when a standard HPLC vial is used for sample injection compared to the Evotip. This highlights the importance of transfer-free sample cleanup, especially after one-pot sample preparation without detrimental adsorptive losses. The highly reproducible peptide separation of the standardized Evosep resulting in high peak capacity allows fast cycling

through relatively wide diaPASEF isolation windows of 25 Th. Improved ionization and ion transfer provided with the brighter ion source of the timsTOF Ultra yields 25% more protein identifications per single cell compared to the timsTOF SCP.

This combination of a reproducible, automated workflow with highly sensitive acquisition allowed us to characterize effects of LPS at the single-cell resolution. For this we used the monocyte cell line THP-1, which are 2-fold smaller in cell diameter compared to HEK293T cells (i.e. 13.7 versus 26.7 µm, respectively). The reduced cell diameter parallels with lower protein identification per single THP-1 cell, as expected. We demonstrate that our proteoCHIP EVO 96 workflow is sufficiently sensitive to recapitulate previously described effect of LPS treatment in these cells. Significantly up-regulated pathways after LPS treatment included pro-inflammatory responses and post-translational modifications of proteins, which are in line with the known function of LPS. Additionally, our workflow reproduces modulations in key LPS-responsive proteins identified in previous studies. Importantly, along with sample preparation capabilities and instrument sensitivity, the cell size highly impacts proteome depth.

To aid wider adoption of single-cell proteomics, we provide detailed methods for both the timsTOF SCP and the timsTOF Ultra, clarifying the impact of peptide separation and acquisition parameters that are crucial to generate quantitative data at high confidence. We highlight that many SCP projects call for increasing the measurement throughput, however, shorter chromatographic gradients directly scale with decreased sensitivity, which retrospectively might impact the ability to make biologically relevant conclusions. We demonstrate that protein identifications are reduced by close to 60% when decreasing the gradient length by 50%. This additionally reduces the overall protein abundance and decreases detection limits by an order of magnitude. As expected, the majority of proteins identified in the 80SPD method are also identified using the 40SPD diaPASEF acquisition method, with comparable relative quantification. We demonstrate that single HEK293T cells acquired on the timsTOF Ultra with the 40SPD chromatographic separation yield on average 4000 protein and span 4 orders of magnitude. This allows us to confidently quantify biologically relevant proteins, such as over 50 ubiquitin ligases, 13 of which are also recovered in the 80SPD method. Therefore, the overall abundance of a protein of interest in a cell line and tissue specific context should be evaluated using publicly available resources such as the Proteome Atlas[66]. Depending on the expected abundance of the protein or proteins of interest, paired with the overall hypothesis, a combinatorial approach of two methods presented here might be most promising. While some projects require in-depth profiling of a few cells, to identify proteins of interest, it is necessary to balance acquisition time and peptide

adsorption during prolonged storage. Other projects with limited sample availability might therefore benefit from reduced depth but rapid acquisition of hundreds or even thousands of single cells using 80SPD. The latter project might benefit from the addition of non-isobaric labels to further increase the throughput, while preserving the proteome depth of 80SPD. The promising combination of multiplexed single cells acquired at 80SPD with minimal missing quantitative values, will drive the application of SCP to more diverse biological questions. This could be especially helpful when profiling sample sets in multiple batches with large inherent biological variability, such as patient material.

Lastly, we adopt normalization approaches previously used for single-cell transcriptomics to minimize technical variability and highlight biological heterogeneity. Importantly, the normalization approach used here does not require a priori information regarding sample identities. Additionally, data analysis across all samples has been performed with a publicly available pan-human library, overcoming the need to generate an experiment-specific library for every project. We consider this specifically important in the analysis of unknown sub-populations or cell-types, which might not be accurately reflected in dedicated libraries. Similarly, the analysis of single cells in combination with higher input samples might impact identification accuracy due to the lack of false discovery rate filtering post-match between runs. In this case, identifications are heavily influenced by the representation of sub-populations within higher input samples.

In conclusion, we have developed and thoroughly evaluated a fully automated label-free SCP sample preparation workflow, composed of commercially available components, that can be implemented by the community using the detailed methods provided. Deep proteomics data acquisition and analysis with high reproducibility was obtained by directly connecting efficient and reproducible chromatography with dedicated MS instrument acquisition parameters and single-cell normalization approaches. The optimization of each step within this SCP workflow allows us to achieve biologically relevant depth and realistic throughput for comprehensive proteome analysis at single cell resolution.

Methods

Cell culture and small molecule treatment

HEK-293T cells were cultured at 37 C and 5% CO_2 in Dulbecco's Modified Eagle's High Glucose media supplemented with 10% Fetal Bovine Serum. Cells were detached with extensive phosphate-buffered saline (PBS) resuspension, cells were pelleted and washed for a total of 3 times. Cells were counted using the Countess™ 3 FL Automated Cell Counter (SN: AMQAF2000,

Invitrogen) and strained using a 5-mL cell strainer tube (SN: 352235, Falcon®) to a final concentration of 200 cells/µL for optimal cell dispensing on the cellenONE®. For the proteome perturbation experiment, HEK-293T cells were seeded in a 6-well plate (Costar® 6-well plates, 3506, Corning Incorporated) at a density of 3 x 10^5 cells/well. THP-1 cells were seeded in a T25 flask at a density of 4 x 10^5 cells/mL in Gibco RPMI media supplemented with 10% Fetal Bovine Serum, Penicillin-Streptomycin and Glutamax. After 8-hours, media was supplemented with LPS (final conc. of 200 ng/mL in DMSO) or DMSO-control. Treatment was carried out for 12-hours prior to cell pelleting, washing, and counting. This was followed by cell straining and subsequent sample processing within the cellenONE.

Sample preparation

The proteoCHIP EVO 96 is a micromachined PTFE plate in the size of a 96-well plate with elevated nanowells to fit on top of a Evotip box as illustrated in Figure 1. For all single cell experiments the conical proteoCHIP EVO 96 wells are manually prefilled with 3µL of Hexadecane, which is solidified during subsequent sample processing at 10C within the cellenONE®. In detail, the proteoCHIP EVO 96 is inserted into the cellenONE® using a dedicated holder (C-PEVO-96-CHB, Scienion, Berlin, Germany), 150nL of master mix (0.2% DDM (D4641-500MG, Sigma-Aldrich, USA/Germany), 100 mM TEAB (17902-500ML, Fluka Analytical, Switzerland), 10 ng/µL trypsin (Promega Gold, V5280, Promega, USA)) is dispensed into each well, cells that match the isolation criteria (gated for cell diameter min. 25 µm and max. 35 µm, circularity 1.1, elongation 1.8) are dispensed to each well, which is followed by a second iteration of 150nL of master mix is dispensed to each well at 80% humidity. The temperature on deck is increased to 45 C during lysis and enzymatic digestion, while continuously rehydrating the samples with 50nL H_2O at 2-minute intervals for 2 hours. Subsequently, sample volume is increased with 3 µL 0.1% formic acid (FA) and 1% Dimethylsulfoxide (DMSO) to simultaneously quench the enzymatic reaction and increase the sample droplet size within the Hexadecane. 1% DMSO is added to the sample, as low concentrations have shown to be beneficial in low-input peptide recovery.[35] Subsequently, the proteoCHIP EVO 96 is transferred to a cooling block for the Hexadecane to solidify again, resulting in complete separation of the sample droplet and the oil before centrifuging to the desired vessel (i.e. 96-well plate or Evotip box) at 1200 rpm for 1 minute. For this, the Evotips are prepared according to manufacturer's instructions, briefly 20µL of 0.1% FA in acetonitrile (ACN - Solvent B) is added to the Evotips using a multichannel pipette and centrifuged at 600 rpm for 1 minute, the Evotips are soaked for 1-2 minutes in 1-propanol, 20µL 0.1% FA (Solvent A) is added to each Evotip and centrifuged at 800 rpm for 1 minute. For sample loading 15µL of Solvent A is added to each Evotip, the proteoCHIP EVO 96 is inverted and aligned on top of the Evotips. The Evotip

box with the inverted proteoCHIP EVO 96 is then centrifuged at 1200 rpm for 1 minute to transfer the sample droplet to the tips. The proteoCHIP EVO 96 is removed and visually inspected that the solidified Hexadecane remained within the nanowells and only the sample droplet was transferred to the Evotips. Subsequently, 150µL of Solvent A is added to each Evotip and centrifuged at 800 rpm for 1 minute to wash the Evotips. Solvent A is then added to the Evotip box to submerge all Evotips and prevent drying of the C18 material. Alternatively, if a 96-well plate (SureSTART™ WebSeal™ 96-Well Microtiter Plate, SN: 60180-P210B, Thermo Fisher Scientific) was used for injection, after SCP sample preparation and oil solidification on the cooling block, the proteoCHIP EVO 96 is inverted and aligned on top of the 96-well plate sample wells. The proteoCHIP EVO 96 and the 96-well plate are taped together and centrifuged at 1200 rpm for 1 minute. Subsequently, the proteoCHIP EVO 96 is inspected for successful removal of the sample droplet from the nanowells and presence of residual Hexadecane within the nanowells. The wells are then sealed with a silicone mat (SureSTART WebSeal 96-Well Plate Sealing Mats, 60180-M210, ThermoFisher) and stored at -20C until injection.

LC MS/MS

Samples were measured on a timsTOF SCP or timsTOF Ultra (Bruker Daltonik Gmbh) with a reversed phase nanoElute (Bruker Daltonik Gmbh), Vanquish Neo (Thermo Fisher Scientific) or Evosep One (Evosep) as indicated. Peptides were separated on the integrated emitter column IonOpticks Aurora Elite (15 cm x 75µM, 1.7µm particle size and 120 Å pore size; AUR3-15075C18-CSI) or Rapid (5cm x 75µM, 1.7µm particle size and 120 Å pore size; AUR3-5075C18-CSI). For both nanoElute and Vanquish Neo, peptides were eluted over a 15-minute gradient ranging from 0-20 Solvent B (0.1% FA in ACN) over 12 minutes and from 20-37 in 2 minutes, at a flow rate of 200nL/min. On the Evosep we used the standard 40SPD or 80SPD methods.

Full MS data were acquired in a range of 100-1700 m/z and 1.3 1/K0 [V-s/cm^{-2}] to 0.6 1/K0 [V-s/cm^{-2}] in diaPASEF. DIA windows range from 400 m/z to 1000 m/z with 25Th isolation windows and were acquired with ramp times of 100ms or otherwise indicated. The collision energy was ramped as a function of increasing mobility starting from 20 eV at 1/K0 [V-s/cm^{-2}] to 60 eV at 1.6 1/K0 [V-s/cm^{-2}]. High sensitivity detection for low sample amounts was enabled without diaPASEF data denoising.

Data analysis

diaPASEF data was analyzed using DIA-NN v1.8.1[67] implemented on the computational platform Terra (https://app.terra.bio/) against a human fractionated library acquired on a timsTOF Pro2 provided by Bruker Daltonics with standard parameters. Briefly, the protease was set to

'Trypsin/P' with one allowed missed cleavage, no allowed variable modifications and oxidized methionine. Peptide length ranges from 7-30 amino acids at precursor charge 1-4 within a m/z range of 300-1800 and fragment ion m/z range of 200-1800. The precursors were filtered for 1% FDR, without MBR at robust LC parameters and retention time-dependent cross-run normalization. Post processing was performed in R, briefly, individual workflow batches were searched separately in DIA-NN and retrospectively combined using their unique Uniprot Accession number and filtered for common laboratory contaminants.

Data completeness for benchmarking experiments detailed in Figure 1 was calculated on the precursor level across the sample set. GRAVY scores were calculated for every distinct peptide sequence identified from the respective condition, based on the Amino Acid Hydropathy Scores[47].

Single-cell samples were grouped using unsupervised (hierarchical) clustering and then normalized using SCnorm[61]. SCnorm groups together proteins that have similar dependence of expression on proteome coverage/depth using quantile regression and then estimates scaling factors within each group of proteins. Additionally, SCnorm allows for the specification of conditions or groups of samples prior to the quantile regression step, such that this normalization approach is applied to each group separately. To group cells, we used an unsupervised clustering approach from the scran package which is based on hierarchical clustering[68]. This clustering groups together cells with similar protein expression patterns prior to the application of SCnorm. The normalized values from SCnorm were $\log_{10}$-transformed and then batch corrected using limma (removeBatchEffect). Drug effects were incorporated into removeBatchEffect as a treatment effect, such that any drug effects were preserved during batch correction (Supplemental Fig. 4). Batch and drug effects were quantified by fitting a linear model between the top 10 principal components and the effect of interest and then calculating the cumulative variance explained across the top 10 principal components (Supplemental Fig. 4). Proteins were filtered for at least 30% data completeness (up to 70% missing values) across all single cells prior to statistical testing.

Moderated two-sample t-tests were performed on the normalized, batch-corrected data using ProTIGY (https://github.com/broadinstitute/protigy). An adjusted p-value of 0.05 (Benajmini-Hochberg) was used as the cutoff for statistical significance. Fold changes are reported as $\log_{10}$-fold changes since the data were originally $\log_{10}$-transformed (Supplemental Table 1). Gene Set Enrichment Analysis (GSEA) was performed on the signed $\log_{10}$ p-values from the two-sample *t*-test using ssGSEA 2.0 (https://github.com/broadinstitute/ssGSEA2.0) on the Reactome gene sets (https://www.gsea-msigdb.org/gsea/msigdb/human/genesets.jsp?collection=CP:REACTOME).

Reactome pathways with adjusted p-value < 0.01 were considered statistically significant (Supplemental Table 1).

Data availability

All mass spectrometry-based proteomics data have been deposited to the MassIVE database with the identifier: MSV000093867 with the password: proteochip.

Acknowledgements

We thank all members of our laboratory for helpful discussions. We specifically want to thank Keith Rivera, Shankha Satpathy, Hasmik Keshishian and Michael Gillette for helpful input on the manuscript. We would like to thank Jonathan Krieger, Sebastian Vaca Jacome, Diego Assis and Matt Willetts from Bruker Daltonics GmbH and Nicholas Bache and Dorte Bekker-Jense from Evosep for their continuous support and essential input to this work. C.C. is a recipient of a SPARC Award from the Broad Institute of MIT & Harvard (#800444) that partially supported this work. This work has been supported in part by grants P01CA206978 to S.A.C from the NIH, U24CA270823, U01CA271402 to S.A.C. and U24-CA271075 to D.R.M. from National Cancer Institute (NCI) Clinical Proteomic Tumor Analysis Consortium program and from the Dr. Miriam and Sheldon G. Adelson Medical Research Foundation to N.D.U. and S.A.C.

Author contributions

B.B. and C.C. prepared and acquired samples. A.S. conceptualized and designed the proteoCHIP. N.M.C. and C.C. performed data analysis. D.R.M., N.D.U., S.A.C. supervised the research, and revised the manuscript.

Conflict of interest

A.S. is an employee of Cellenion. S.A.C. is a member of the scientific advisory boards of Kymera, PTM BioLabs, Seer and PrognomIQ.

References

1. Djebali, S., Davis, C.A., Merkel, A., Dobin, A., Lassmann, T., Mortazavi, A., Tanzer, A., Lagarde, J., Lin, W., Schlesinger, F., et al. (2012). Landscape of transcription in human cells. Nature *489*, 101–108. 10.1038/nature11233.

2. Thul, P.J., Åkesson, L., Wiking, M., Mahdessian, D., Geladaki, A., Blal, H.A., Alm, T., Asplund, A., Björk, L., Breckels, L.M., et al. (2017). A subcellular map of the human proteome. Science *356*. 10.1126/science.aal3321.

3. Izar, B., Tirosh, I., Stover, E.H., Wakiro, I., Cuoco, M.S., Alter, I., Rodman, C., Leeson, R., Su, M.-J., Shah, P., et al. (2020). A single-cell landscape of high-grade serous ovarian cancer. Nature Medicine *26*, 1271–1279. 10.1038/s41591-020-0926-0.

4. Wang, X., Allen, W.E., Wright, M.A., Sylwestrak, E.L., Samusik, N., Vesuna, S., Evans, K., Liu, C., Ramakrishnan, C., Liu, J., et al. (2018). Three-dimensional intact-tissue sequencing of single-cell transcriptional states. Science *361*. 10.1126/science.aat5691.

5. Rosenberger, F.A., Thielert, M., Strauss, M.T., Schweizer, L., Ammar, C., Mädler, S.C., Metousis, A., Skowronek, P., Wahle, M., Madden, K., et al. (2023). Spatial single-cell mass spectrometry defines zonation of the hepatocyte proteome. Nat Methods *20*, 1530–1536. 10.1038/s41592-023-02007-6.

6. Ctortecka, C., and Mechtler, K. The rise of single-cell proteomics. Analytical Science Advances *n/a*. https://doi.org/10.1002/ansa.202000152.

7. Budnik, B., Levy, E., Harmange, G., and Slavov, N. (2018). SCoPE-MS: mass spectrometry of single mammalian cells quantifies proteome heterogeneity during cell differentiation. Genome Biology *19*. 10.1186/s13059-018-1547-5.

8. Schoof, E.M., Furtwängler, B., Üresin, N., Rapin, N., Savickas, S., Gentil, C., Lechman, E., Keller, U. auf dem, Dick, J.E., and Porse, B.T. (2021). Quantitative single-cell proteomics as a tool to characterize cellular hierarchies. Nat Commun *12*, 3341. 10.1038/s41467-021-23667-y.

9. Zhu, Y., Clair, G., Chrisler, W.B., Shen, Y., Zhao, R., Shukla, A.K., Moore, R.J., Misra, R.S., Pryhuber, G.S., Smith, R.D., et al. (2018). Proteomic Analysis of Single Mammalian Cells Enabled by Microfluidic Nanodroplet Sample Preparation and Ultrasensitive NanoLC-MS. Angewandte Chemie International Edition *57*, 12370–12374. 10.1002/anie.201802843.

10. Brunner, A.-D., Thielert, M., Vasilopoulou, C., Ammar, C., Coscia, F., Mund, A., Hoerning, O.B., Bache, N., Apalategui, A., Lubeck, M., et al. (2022). Ultra-high sensitivity mass spectrometry quantifies single-cell proteome changes upon perturbation. Molecular Systems Biology *18*, e10798. 10.15252/msb.202110798.

11. Li, Z.-Y., Huang, M., Wang, X.-K., Zhu, Y., Li, J.-S., Wong, C.C.L., and Fang, Q. (2018). Nanoliter-Scale Oil-Air-Droplet Chip-Based Single Cell Proteomic Analysis. Analytical Chemistry *90*, 5430–5438. 10.1021/acs.analchem.8b00661.

12. Olsen, J.V., and Mann, M. (2013). Status of Large-scale Analysis of Post-translational Modifications by Mass Spectrometry. Mol Cell Proteomics *12*, 3444–3452. 10.1074/mcp.O113.034181.

13. Aebersold, R., and Mann, M. (2016). Mass-spectrometric exploration of proteome structure and function. Nature *537*, 347–355. 10.1038/nature19949.

14. Wiśniewski, J.R., Hein, M.Y., Cox, J., and Mann, M. (2014). A “Proteomic Ruler” for Protein Copy Number and Concentration Estimation without Spike-in Standards. Mol Cell Proteomics *13*, 3497–3506. 10.1074/mcp.M113.037309.

15. Derks, J., Leduc, A., Wallmann, G., Huffman, R.G., Willetts, M., Khan, S., Specht, H., Ralser, M., Demichev, V., and Slavov, N. (2022). Increasing the throughput of sensitive proteomics by plexDIA. Nat Biotechnol, 1–10. 10.1038/s41587-022-01389-w.

16. Furtwängler, B., Üresin, N., Motamedchaboki, K., Huguet, R., Lopez-Ferrer, D., Zabrouskov, V., Porse, B.T., and Schoof, E.M. (2022). Real-Time Search-Assisted Acquisition on a Tribrid Mass Spectrometer Improves Coverage in Multiplexed Single-Cell Proteomics. Molecular & Cellular Proteomics *21*, 100219. 10.1016/j.mcpro.2022.100219.

17. Specht, H., Emmott, E., Petelski, A.A., Huffman, R.G., Perlman, D.H., Serra, M., Kharchenko, P., Koller, A., and Slavov, N. (2021). Single-cell proteomic and transcriptomic analysis of macrophage heterogeneity using SCoPE2. Genome Biology *22*, 50. 10.1186/s13059-021-02267-5.

18. Ctortecka, C., Hartlmayr, D., Seth, A., Mendjan, S., Tourniaire, G., Udeshi, N.D., Carr, S.A., and Mechtler, K. (2023). An automated nanowell-array workflow for quantitative multiplexed single-cell proteomics sample preparation at high sensitivity. Molecular & Cellular Proteomics *0*. 10.1016/j.mcpro.2023.100665.

19. Woo, J., Clair, G.C., Williams, S.M., Feng, S., Tsai, C.-F., Moore, R.J., Chrisler, W.B., Smith, R.D., Kelly, R.T., Paša-Tolić, L., et al. (2022). Three-dimensional feature matching improves coverage for single-cell proteomics based on ion mobility filtering. Cell Systems *13*, 426-434.e4. 10.1016/j.cels.2022.02.003.

20. Ctortecka, C., Krššáková, G., Stejskal, K., Penninger, J.M., Mendjan, S., Mechtler, K., and Stadlmann, J. (2021). Comparative proteome signatures of trace samples by multiplexed Data-Independent Acquisition. Molecular & Cellular Proteomics *0*. 10.1016/j.mcpro.2021.100177.

21. Cong, Y., Liang, Y., Motamedchaboki, K., Huguet, R., Truong, T., Zhao, R., Shen, Y., Lopez-Ferrer, D., Zhu, Y., and Kelly, R.T. (2020). Improved Single-Cell Proteome Coverage Using Narrow-Bore Packed NanoLC Columns and Ultrasensitive Mass Spectrometry. Analytical Chemistry *92*, 2665–2671. 10.1021/acs.analchem.9b04631.

22. Zheng, R., Matzinger, M., Mayer, R.L., Valenta, A., Sun, X., and Mechtler, K. (2023). A High-Sensitivity Low-Nanoflow LC-MS Configuration for High-Throughput Sample-Limited Proteomics. Anal. Chem. *95*, 18673–18678. 10.1021/acs.analchem.3c03058.

23. Webber, K.G.I., Truong, T., Johnston, S.M., Zapata, S.E., Liang, Y., Davis, J.M., Buttars, A.D., Smith, F.B., Jones, H.E., Mahoney, A.C., et al. (2022). Label-Free Profiling of up to 200

Single-Cell Proteomes per Day Using a Dual-Column Nanoflow Liquid Chromatography Platform. Anal. Chem. 10.1021/acs.analchem.2c00646.

24. Huffman, R.G., Leduc, A., Wichmann, C., Gioia, M. di, Borriello, F., Specht, H., Derks, J., Khan, S., Khoury, L., Emmott, E., et al. (2022). Prioritized single-cell proteomics reveals molecular and functional polarization across primary macrophages. Preprint at bioRxiv, 10.1101/2022.03.16.484655 10.1101/2022.03.16.484655.

25. Petrosius, V., Aragon-Fernandez, P., Üresin, N., Kovacs, G., Phlairaharn, T., Furtwängler, B., Op De Beeck, J., Skovbakke, S.L., Goletz, S., Thomsen, S.F., et al. (2023). Exploration of cell state heterogeneity using single-cell proteomics through sensitivity-tailored data-independent acquisition. Nat Commun *14*, 5910. 10.1038/s41467-023-41602-1.

26. Ctortecka, C., Stejskal, K., Krššáková, G., Mendjan, S., and Mechtler, K. (2021). Quantitative Accuracy and Precision in Multiplexed Single-Cell Proteomics. Anal. Chem., acs.analchem.1c04174. 10.1021/acs.analchem.1c04174.

27. Cheung, T.K., Lee, C.-Y., Bayer, F.P., McCoy, A., Kuster, B., and Rose, C.M. (2020). Defining the carrier proteome limit for single-cell proteomics. Nature Methods, 1–8. 10.1038/s41592-020-01002-5.

28. Ye, Z., Batth, T.S., Rüther, P., and Olsen, J.V. (2022). A deeper look at carrier proteome effects for single-cell proteomics. Commun Biol *5*, 1–8. 10.1038/s42003-022-03095-4.

29. Savitski, M.M., Mathieson, T., Zinn, N., Sweetman, G., Doce, C., Becher, I., Pachl, F., Kuster, B., and Bantscheff, M. (2013). Measuring and Managing Ratio Compression for Accurate iTRAQ/TMT Quantification. Journal of Proteome Research *12*, 3586–3598. 10.1021/pr400098r.

30. Madern, M., Reiter, W., Stanek, F., Hartl, N., Mechtler, K., and Hartl, M. (2022). A causal model of ion interference enables assessment and correction of ratio compression in multiplex proteomics. Preprint at bioRxiv, 10.1101/2022.06.24.497446 10.1101/2022.06.24.497446.

31. Ow, S.Y., Salim, M., Noirel, J., Evans, C., and Wright, P.C. (2011). Minimising iTRAQ ratio compression through understanding LC-MS elution dependence and high-resolution HILIC fractionation. PROTEOMICS *11*, 2341–2346. https://doi.org/10.1002/pmic.201000752.

32. Matzinger, M., Müller, E., Dürnberger, G., Pichler, P., and Mechtler, K. (2023). Robust and Easy-to-Use One-Pot Workflow for Label-Free Single-Cell Proteomics. Anal. Chem. *95*, 4435–4445. 10.1021/acs.analchem.2c05022.

33. Truong, T., Webber, K.G.I., Madisyn Johnston, S., Boekweg, H., Lindgren, C.M., Liang, Y., Nydegger, A., Xie, X., Tsang, T.-M., Jayatunge, D.A.D.N., et al. (2023). Data-Dependent Acquisition with Precursor Coisolation Improves Proteome Coverage and Measurement Throughput for Label-Free Single-Cell Proteomics**. Angewandte Chemie *135*, e202303415. 10.1002/ange.202303415.

34. Johnston, S.M., Webber, K.G.I., Xie, X., Truong, T., Nydegger, A., Lin, H.-J.L., Nwosu, A., Zhu, Y., and Kelly, R.T. (2023). Rapid, One-Step Sample Processing for Label-Free Single-Cell Proteomics. J. Am. Soc. Mass Spectrom. *34*, 1701–1707. 10.1021/jasms.3c00159.

35. O'Connell, J.D., Paulo, J.A., O'Brien, J.J., and Gygi, S.P. (2018). Proteome-wide evaluation of two common protein quantification methods. J. Proteome Res. 10.1021/acs.jproteome.8b00016.

36. Bache, N., Geyer, P.E., Bekker-Jensen, D.B., Hoerning, O., Falkenby, L., Treit, P.V., Doll, S., Paron, I., Müller, J.B., Meier, F., et al. (2018). A Novel LC System Embeds Analytes in Pre-formed Gradients for Rapid, Ultra-robust Proteomics. Molecular & Cellular Proteomics *17*, 2284–2296. 10.1074/mcp.TIR118.000853.

37. Thielert, M., Itang, E.C., Ammar, C., Rosenberger, F.A., Bludau, I., Schweizer, L., Nordmann, T.M., Skowronek, P., Wahle, M., Zeng, W.-F., et al. (2023). Robust dimethyl-based multiplex-DIA doubles single-cell proteome depth via a reference channel. Molecular Systems Biology *n/a*, e11503. 10.15252/msb.202211503.

38. Meier, F., Brunner, A.-D., Frank, M., Ha, A., Bludau, I., Voytik, E., Kaspar-Schoenefeld, S., Lubeck, M., Raether, O., Bache, N., et al. (2020). diaPASEF: parallel accumulation–serial fragmentation combined with data-independent acquisition. Nature Methods *17*, 1229–1236. 10.1038/s41592-020-00998-0.

39. Venable, J.D., Dong, M.-Q., Wohlschlegel, J., Dillin, A., and Yates, J.R. (2004). Automated approach for quantitative analysis of complex peptide mixtures from tandem mass spectra. Nature Methods *1*, 39–45. 10.1038/nmeth705.

40. Gillet, L.C., Navarro, P., Tate, S., Röst, H., Selevsek, N., Reiter, L., Bonner, R., and Aebersold, R. (2012). Targeted Data Extraction of the MS/MS Spectra Generated by Data-independent Acquisition: A New Concept for Consistent and Accurate Proteome Analysis. Molecular & Cellular Proteomics *11*. 10.1074/mcp.O111.016717.

41. Stejskal, K., Op de Beeck, J., Dürnberger, G., Jacobs, P., and Mechtler, K. (2021). Ultrasensitive NanoLC-MS of Subnanogram Protein Samples Using Second Generation Micropillar Array LC Technology with Orbitrap Exploris 480 and FAIMS PRO. Anal. Chem. *93*, 8704–8710. 10.1021/acs.analchem.1c00990.

42. Leduc, A., Huffman, R.G., Cantlon, J., Khan, S., and Slavov, N. (2022). Exploring functional protein covariation across single cells using nPOP. Genome Biology *23*, 261. 10.1186/s13059-022-02817-5.

43. Ye, Z., Sabatier, P., Hoeven, L., Phlairaharn, T., Hartlmayr, D., Izaguirre, F., Seth, A., Joshi, H., Bekker-Jensen, D., Bache, N., et al. (2023). High-throughput and scalable single cell proteomics identifies over 5000 proteins per cell (Systems Biology) 10.1101/2023.11.27.568953.

44. Williams, S.M., Liyu, A.V., Tsai, C.-F., Moore, R.J., Orton, D.J., Chrisler, W.B., Gaffrey, M.J., Liu, T., Smith, R.D., Kelly, R.T., et al. (2020). Automated Coupling of Nanodroplet Sample Preparation with Liquid Chromatography-Mass Spectrometry for High-Throughput Single-Cell Proteomics. Analytical Chemistry. 10.1021/acs.analchem.0c01551.

45. Ye, Z., Sabatier, P., Martin-Gonzalez, J., Eguchi, A., Bekker-Jensen, D.B., Bache, N., and Olsen, J.V. (2023). One-Tip enables comprehensive proteome coverage in minimal cells and single zygotes. Preprint at bioRxiv, 10.1101/2023.08.10.552756 10.1101/2023.08.10.552756.

46. Makhmut, A., Qin, D., Hartlmayr, D., Seth, A., and Coscia, F. (2023). An automated and fast sample preparation workflow for laser microdissection guided ultrasensitive proteomics (Systems Biology) 10.1101/2023.11.29.569257.

47. Kyte, J., and Doolittle, R.F. (1982). A simple method for displaying the hydropathic character of a protein. Journal of Molecular Biology *157*, 105–132. 10.1016/0022-2836(82)90515-0.

48. Bruker Daltonik (2023). 1901442-timstof-ultra-ebook-rev2.pdf. https://www.bruker.com/en/products-and-solutions/mass-spectrometry/timstof.html.

49. Yu, F., Haynes, S.E., and Nesvizhskii, A.I. (2021). IonQuant Enables Accurate and Sensitive Label-Free Quantification With FDR-Controlled Match-Between-Runs. Molecular & Cellular Proteomics *20*, 100077. 10.1016/j.mcpro.2021.100077.

50. Lim, M.Y., Paulo, J.A., and Gygi, S.P. (2019). Evaluating False Transfer Rates from the Match-Between-Runs Algorithm with a Two-Proteome Model. J. Proteome Res., 4020–4026. 10.1021/acs.jproteome.9b00492.

51. Hershko, A., and Ciechanover, A. (1998). The Ubiquitin System. Annual Review of Biochemistry *67*, 425–479. 10.1146/annurev.biochem.67.1.425.

52. Zheng, N., and Shabek, N. (2017). Ubiquitin Ligases: Structure, Function, and Regulation. Annual Review of Biochemistry *86*, 129–157. 10.1146/annurev-biochem-060815-014922.

53. Kirkin, V., and Dikic, I. (2011). Ubiquitin networks in cancer. Current Opinion in Genetics & Development *21*, 21–28. 10.1016/j.gde.2010.10.004.

54. Krönke, J., Udeshi, N.D., Narla, A., Grauman, P., Hurst, S.N., McConkey, M., Svinkina, T., Heckl, D., Comer, E., Li, X., et al. (2014). Lenalidomide Causes Selective Degradation of IKZF1 and IKZF3 in Multiple Myeloma Cells. Science *343*, 301–305. 10.1126/science.1244851.

55. Seim, G.L., Britt, E.C., John, S.V., Yeo, F.J., Johnson, A.R., Eisenstein, R.S., Pagliarini, D.J., and Fan, J. (2019). Two-stage metabolic remodelling in macrophages in response to lipopolysaccharide and interferon-γ stimulation. Nat Metab *1*, 731–742. 10.1038/s42255-019-0083-2.

56. Mulvey, C.M., Breckels, L.M., Crook, O.M., Sanders, D.J., Ribeiro, A.L.R., Geladaki, A., Christoforou, A., Britovšek, N.K., Hurrell, T., Deery, M.J., et al. (2021). Spatiotemporal proteomic profiling of the pro-inflammatory response to lipopolysaccharide in the THP-1 human leukaemia cell line. Nat Commun *12*, 5773. 10.1038/s41467-021-26000-9.

57. Yücel, G., Zhao, Z., El-Battrawy, I., Lan, H., Lang, S., Li, X., Buljubasic, F., Zimmermann, W.-H., Cyganek, L., Utikal, J., et al. (2017). Lipopolysaccharides induced inflammatory responses and electrophysiological dysfunctions in human-induced pluripotent stem cell derived cardiomyocytes. Sci Rep *7*, 2935. 10.1038/s41598-017-03147-4.

58. Widdrington, J.D., Gomez-Duran, A., Pyle, A., Ruchaud-Sparagano, M.-H., Scott, J., Baudouin, S.V., Rostron, A.J., Lovat, P.E., Chinnery, P.F., and Simpson, A.J. (2018). Exposure of Monocytic Cells to Lipopolysaccharide Induces Coordinated Endotoxin

Tolerance, Mitochondrial Biogenesis, Mitophagy, and Antioxidant Defenses. Frontiers in Immunology *9*.

59. Vallejos, C.A., Risso, D., Scialdone, A., Dudoit, S., and Marioni, J.C. (2017). Normalizing single-cell RNA sequencing data: challenges and opportunities. Nat Methods *14*, 565–571. 10.1038/nmeth.4292.

60. Clark, N.M., Elmore, J.M., and Walley, J.W. (2022). To the proteome and beyond: advances in single-cell omics profiling for plant systems. Plant Physiology *188*, 726–737. 10.1093/plphys/kiab429.

61. Bacher, R., Chu, L.-F., Leng, N., Gasch, A.P., Thomson, J.A., Stewart, R.M., Newton, M., and Kendziorski, C. (2017). SCnorm: robust normalization of single-cell RNA-seq data. Nat Methods *14*, 584–586. 10.1038/nmeth.4263.

62. Subramanian, A., Tamayo, P., Mootha, V.K., Mukherjee, S., Ebert, B.L., Gillette, M.A., Paulovich, A., Pomeroy, S.L., Golub, T.R., Lander, E.S., et al. (2005). Gene set enrichment analysis: A knowledge-based approach for interpreting genome-wide expression profiles. Proceedings of the National Academy of Sciences *102*, 15545–15550. 10.1073/pnas.0506580102.

63. Ubanako, P., Xelwa, N., and Ntwasa, M. (2019). LPS induces inflammatory chemokines via TLR-4 signalling and enhances the Warburg Effect in THP-1 cells. PLoS One *14*, e0222614. 10.1371/journal.pone.0222614.

64. Dobashi, K., Aihara, M., Araki, T., Shimizu, Y., Utsugi, M., Iizuka, K., Murata, Y., Hamuro, J., Nakazawa, T., and Mori, M. (2001). Regulation of LPS induced IL-12 production by IFN-γ and IL-4 through intracellular glutathione status in human alveolar macrophages. Clin Exp Immunol *124*, 290–296. 10.1046/j.1365-2249.2001.01535.x.

65. Italiani, P., Mazza, E.M.C., Lucchesi, D., Cifola, I., Gemelli, C., Grande, A., Battaglia, C., Bicciato, S., and Boraschi, D. (2014). Transcriptomic Profiling of the Development of the Inflammatory Response in Human Monocytes In Vitro. PLoS One *9*, e87680. 10.1371/journal.pone.0087680.

66. Regev, A., Teichmann, S.A., Lander, E.S., Amit, I., Benoist, C., Birney, E., Bodenmiller, B., Campbell, P., Carninci, P., Clatworthy, M., et al. The Human Cell Atlas. eLife *6*, e27041. 10.7554/eLife.27041.

67. Demichev, V., Messner, C.B., Vernardis, S.I., Lilley, K.S., and Ralser, M. (2020). DIA-NN: neural networks and interference correction enable deep proteome coverage in high throughput. Nature Methods *17*, 41–44. 10.1038/s41592-019-0638-x.

68. L. Lun, A.T., Bach, K., and Marioni, J.C. (2016). Pooling across cells to normalize single-cell RNA sequencing data with many zero counts. Genome Biology *17*, 75. 10.1186/s13059-016-0947-7.